

On the non-linear vibrations of clamped-free cylindrical shells subjected to combined loads

Zenón José Guzmán Nuñez Del Prado and Lamartine Brasil Alves Santos Junior

*School of Civil and Environmental Engineering, Federal University of Goiás
Av. Universitária, 1488, St. Universitário, 74605-220, Goiânia, GO, Brazil
zenon@ufg.br – lamartine.brasil@discente.ufg.br*

Abstract. In this work, the nonlinear vibrations of clamped-free cylindrical shells subjected to combined loads is studied. Combined loads such as axial, lateral and base acceleration can generate complex vibrations in shells and its combination is important to consider in project of these kind of structures. For this, to model the shell the Koiter – Sanders nonlinear shell theory is considered, and the Rayleigh-Ritz method is applied to obtain a set of non-linear dynamic equations which are solved in turn by the fourth order Runge-Kutta method. To study the nonlinear dynamic response, an expansion with fifteen degrees of freedom in the axial, radial and lateral directions, which represents the correct modal coupling, is considered. The nonlinear static paths, the parametric instability boundaries, resonance curves and Poincaré maps are obtained. It is possible to observe that, depending on the geometry ratios, the intensity of the loads, the shell will display complex nonlinear response showing softening, chaotic or quasi-periodic oscillations.

Keywords: cylindrical shells, nonlinear vibrations, combined load effect.

1 Introduction

Due to its high capability to strength external and internal forces, circular cylindrical shells can be found in several engineering areas and in literature, it is possible to find a large amount of works related to linear and nonlinear analysis of simply supported cylindrical shells but, works related to clamped-free boundary conditions are very scarce. Linear vibrations of clamped-free cylindrical shell have been previously studied [1-3] but, there is a reduced number for nonlinear vibrations, one of the most famous work is due to Chiba [4,5] who studied experimentally the nonlinear free vibrations of polyester shells and, recently, Kurylov and Amabili [6] who, using the Chebyshev polynomials to expand the displacement fields, studied the forced nonlinear vibrations of clamped-free cylindrical shells. The main difficulty in all studies is to find the correct expansions to discretize the fields displacements for nonlinear analysis.

In this work, the nonlinear vibrations of clamped-free cylindrical shells subjected to both axial and partial lateral loads are studied. For this, to model the shell the Koiter – Sanders nonlinear shell theory is considered, and the Rayleigh-Ritz method is applied to obtain a set of non-linear dynamic equations which are solved in turn by the fourth order Runge-Kutta method. To study the nonlinear dynamic response, an expansion with fifteen degrees of freedom in the axial, radial and lateral directions, which represents the correct modal coupling, is considered.

2 Mathematical Formulation

Consider a perfect clamped-free elastic cylindrical shell with radius R , thickness h , length L , density ρ , Young modulus E and Poisson coefficient ν and subjected to an axial static and harmonic load $P_{ax}(t) = P_0 + P_1 \cos(\Omega_{ax}t)$ and a lateral harmonic load $F_{lat}(t) = F_L R h^2 \rho \omega^2 \cos(\Omega_{lat}t)$ acting along heigh H_L as seen in Fig. 1. The field displacements of the middle surface of the shell are in the axial $u(x, \theta, t)$, radial $v(x, \theta, t)$ and lateral $w(x, \theta, t)$ directions, respectively where x and θ are the axial and radial coordinates and t is the time.

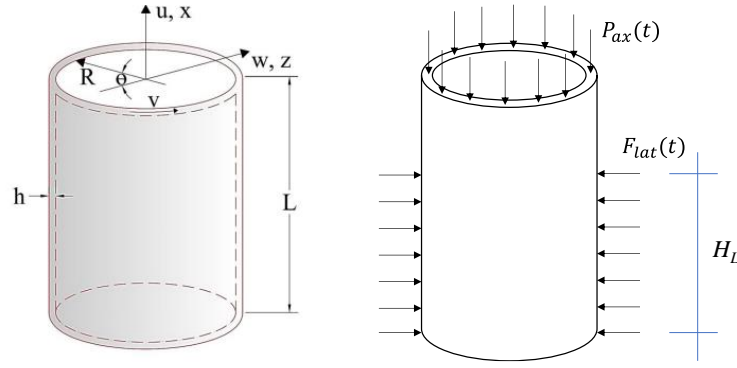


Figure 1. Geometry and coordinates of cylindrical shell.

The strain relations of the cylindrical shell can be written as $\varepsilon_x = \varepsilon_{x,0} + zk_x$, $\varepsilon_\theta = \varepsilon_{\theta,0} + zk_\theta$, $\gamma_{x\theta} = \gamma_{x\theta,0} + zk_{x\theta}$ where z is the distance of the arbitrary point of the shell from the middle surface.

The middle surface strain–displacement relations, changes of curvature and torsion according to Sanders–Koiter nonlinear shell theory are given by:

$$\varepsilon_{x,0} = \frac{\partial u}{\partial x} + \frac{1}{2} \left(\frac{\partial w}{\partial x} \right)^2 + \frac{1}{8} \left(\frac{\partial v}{\partial x} - \frac{\partial u}{R \partial \theta} \right)^2 \quad (1)$$

$$\varepsilon_{\theta,0} = \frac{\partial v}{R \partial \theta} + \frac{w}{R} + \frac{1}{2} \left(\frac{\partial w}{R \partial \theta} - \frac{v}{R} \right)^2 + \frac{1}{8} \left(\frac{\partial u}{R \partial \theta} - \frac{\partial v}{\partial x} \right)^2 \quad (2)$$

$$\gamma_{x\theta,0} = \frac{\partial u}{R \partial \theta} + \frac{\partial v}{\partial x} + \frac{\partial w}{\partial x} \left(\frac{\partial w}{R \partial \theta} - \frac{v}{R} \right) \quad (3)$$

$$k_x = -\frac{\partial^2 w}{\partial x^2}, \quad k_\theta = \frac{\partial v}{R^2 \partial \theta} - \frac{\partial^2 w}{R^2 \partial \theta^2}, \quad k_{x\theta} = -2 \frac{\partial^2 w}{R \partial x \partial \theta} + \frac{1}{2R} \left(3 \frac{\partial v}{\partial x} - \frac{\partial u}{R \partial \theta} \right) \quad (4)$$

The elastic strain energy, neglecting σ_z for plane stress, is given by [2]

$$U = \frac{1}{2} R \int_0^{2\pi} \int_0^L \int_{-h/2}^{h/2} (\sigma_x \varepsilon_x + \sigma_\theta \varepsilon_\theta + \tau_{x\theta} \gamma_{x\theta}) dx (1 + z/R) d\theta dz \quad (5)$$

where stress-strain relations are given by:

$$\sigma_x = \frac{E}{1 - \nu^2} (\varepsilon_x + \nu \varepsilon_\theta), \quad \sigma_\theta = \frac{E}{1 - \nu^2} (\varepsilon_\theta + \nu \varepsilon_x), \quad \tau_{x\theta} = \frac{E}{2(1 + \nu)} \gamma_{x\theta} \quad (6)$$

The kinetic energy, considering only translational inertia, is given by:

$$T = \frac{1}{2} \rho h R \int_0^{2\pi} \int_0^L (\dot{u}^2 + \dot{v}^2 + \dot{w}^2) dx d\theta \quad (7)$$

The work of external forces is:

$$W = R \int_0^{2\pi} \int_0^L \{ [P_{ax}(\delta(x-0) - \delta(x-L))]u + F_{lat}(t)[H(x-0) - H(x-H_L)]w \} dx d\theta \quad (8)$$

Where δ and H are the Dirac and Heaviside functions, respectively.

Finally, the work of nonconservative forces is:

$$F = \frac{1}{2} c R \int_0^{2\pi} \int_0^L (\dot{u}^2 + \dot{v}^2 + \dot{w}^2) dx d\theta \quad (9)$$

where c is the viscous damping coefficient.

The field displacements can be expanded as:

$$\begin{aligned}
w(x, \theta, t) &= \sum_{m=1}^M \sum_{n=1}^N h \beta(m, x) [q_{m,n,d}(t) \cos(n\theta) + q_{m,n,c}(t) \sin(n\theta)] \\
u(x, \theta, t) &= \sum_{m=1}^M \sum_{n=1}^N h \beta_1(m, x) [q_{m,n,d}(t) \cos(n\theta) + q_{m,n,c}(t) \sin(n\theta)] \\
v(x, \theta, t) &= \sum_{m=1}^M \sum_{n=0}^N h \beta(m, x) [q_{m,n,d}(t) \sin(n\theta) + q_{m,n,c}(t) \cos(n\theta)]
\end{aligned} \tag{10}$$

With

$$\beta(m, x) = 1 - \cos \left[\frac{1(2m-1)\pi x}{2L} \right], \quad \beta_1(m, x) = \sin \left[\frac{1(2m-1)\pi x}{2L} \right] \tag{11}$$

where m is the axial half-wave number, n is the circumferential wavenumber, subscript d refers to driven mode and subscript c refers to companion mode.

The boundary conditions of a clamped-free cylindrical shell are given by:

$$u = v = w = \frac{\partial w}{\partial x} = 0 \text{ at } x = 0 \text{ and } N_x = N_{x\theta} + \frac{M_{x\theta}}{R} = M_x = Q_x + \frac{\partial M_{x\theta}}{R \partial \theta} = 0 \text{ at } x = L \tag{12}$$

Substituting the field displacements of Eq. (10) in Eq. (14), the set of nonlinear equations of dynamic equilibrium can be obtained.

$$\frac{d}{dt} \left(\frac{\partial T}{\partial \dot{q}_i} \right) + \frac{\partial U}{\partial q_i} = - \frac{\partial F}{\partial \dot{q}_i} + \frac{\partial W}{\partial q_i}, \quad i = 1, \dots, \text{dof} \tag{13}$$

where $q_i = [u_{1,0}, u_{2,0}, \dots, u_{1,n,d}, u_{2,n,d}, \dots, v_{1,0}, v_{2,0}, \dots, v_{1,n,d}, v_{2,n,d}, \dots, w_{1,0}, w_{2,0}, \dots, w_{1,n,d}, w_{2,n,d}, \dots]$.

3 Numerical Results.

Three different clamped-free cylindrical shell geometries were considered and, all of them with Young's modulus $E = 4.65e9 \text{ N/m}^2$, density $\rho = 1400 \text{ kg/m}^3$ and Poisson coefficient $\nu = 0.38$. Table 1 displays the selected shell geometries and L/R and R/h ratios. First, in order to obtain the natural frequency, a linear free vibrations analysis was performed considering the following field displacements (without companion mode) $u = (1,0) + (2,0) + (3,0) + \dots + (1,n) + (2,n) + (3,n) + \dots$, $v = (1,0) + (2,0) + (3,0) + \dots + (1,n) + (2,n) + (3,n) + \dots$ and $w = (1,0) + (2,0) + (3,0) + \dots + (1,n) + (2,n) + (3,n) + \dots$. Table 1 also shows the natural frequency and corresponding (m,n) for each shell geometry as well as the corresponding critical axial load.

Table 1. Selected shell geometries.

Geometry	L (m)	R (m)	h (mm)	L/R	R/h	P_{cr} (N)	ω_0 (rad/sec)	(m,n)
01	0.48	0.24	0.254	2.0	944	231.36	179.165	(1,7)
02	0.72	0.24	0.300	3.0	800	326.09	130.728	(1,6)
03	0.24	0.24	1.200	1.0	200	4621.08	757.200	(1,7)

For the nonlinear analysis of the shell, the correct field displacements showing the coupling and modal interaction displaying softening behavior should be considered. For this, five field displacements without considering the companion mode were selected and are showed in Table 2. As can be seen, field displacements with eighteen, sixteen and fifteen degrees of freedom, containing symmetrical and axy-symmetrical modes, were selected.

Figure 2 shows the normalized frequency-amplitude relations for Geometry 01 and obtained for each modal expansion. As can be observed, all curves display softening behavior and to study which expansion generates the best nonlinear response, they were compared with experimental results obtained by Chiba (1993). As can be observed, the curve obtained with expansion named 15a generates the closest curve to experimental result and it will be considered in the nonlinear vibration analysis.

Table 1. Selected field displacements

Modal Expansion	
18a	$w = q_1h(1,n) + q_2h(1,2n) + q_3h(2,n) + q_4h(2,2n) + q_5h(1,0) + q_6h(2,0) + hq_7(3,0)$ $u = q_8h(1,n) + q_9h(1,2n) + q_{10}h(2,n) + q_{11}h(2,2n) + q_{12}h(1,0) + q_{13}h(2,0) + q_{14}h(3,0)$ $v = q_{15}h(1,n) + q_{16}h(1,2n) + q_{17}h(2,n) + q_{18}h(2,2n)$
18b	$w = q_1h(1,n) + q_2h(1,2n) + q_3h(2,2n) + q_4h(3,2n) + q_5h(1,0) + q_6h(2,0) + hq_7(3,0)$ $u = q_8h(1,n) + q_9h(1,2n) + q_{10}h(2,2n) + q_{11}h(3,2n) + q_{12}h(1,0) + q_{13}h(2,0) + q_{14}h(3,0)$ $v = q_{15}h(1,n) + q_{16}h(1,2n) + q_{17}h(2,2n) + q_{18}h(3,2n)$
16c	$w = q_1h(1,n) + q_2h(1,2n) + q_3h(1,3n) + q_4h(2,2n) + q_5h(1,0) + hq_6(2,0)$ $u = q_7h(1,n) + q_8h(1,2n) + q_9h(1,3n) + q_{10}h(2,2n) + q_{11}h(1,0) + q_{12}h(2,0)$ $v = q_{13}h(1,n) + q_{14}h(1,2n) + q_{15}h(1,3n) + q_{16}h(2,2n)$
15a	$w = q_1h(1,n) + q_2h(1,2n) + q_3h(2,2n) + q_4h(1,0) + q_5h(2,0) + hq_6(3,0)$ $u = q_7h(1,n) + q_8h(1,2n) + q_9h(2,2n) + q_{10}h(1,0) + q_{11}h(2,0) + q_{12}h(3,0)$ $v = q_{13}h(1,n) + q_{14}h(1,2n) + q_{15}h(1,3n)$
15c	$w = q_1h(1,n) + q_2h(1,2n) + q_3h(2,2n) + q_4h(1,0) + q_5h(2,0) + hq_6(3,0)$ $u = q_7h(1,n) + q_8h(1,2n) + q_9h(2,2n) + q_{10}h(1,0) + q_{11}h(2,0) + q_{12}h(3,0)$ $v = q_{13}h(1,n) + q_{14}h(1,2n) + q_{15}h(2,2n)$

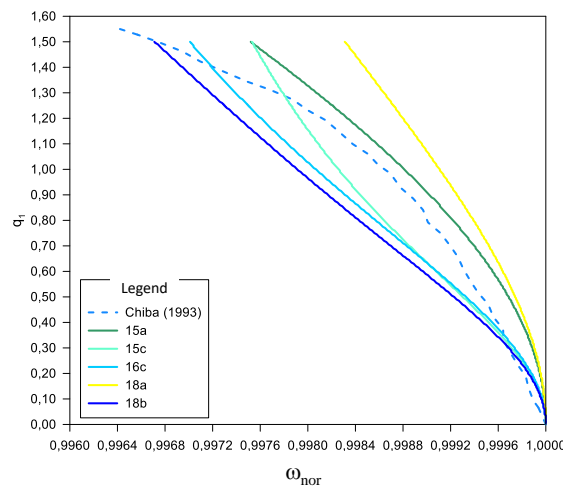


Figure 2. Frequency-amplitude relations for selected field displacement expansions.

The nonlinear post-critical paths of static axial load were obtained applying the Newton-Raphson method and they were plotted to analyze the influence of geometry relations on the nonlinear static paths of the shells. Figure 3 depicts the nonlinear paths for each geometry and as can be seen, it is possible to observe that all curves display softening behavior after critical load and a turning point with hardening behavior. Geometry ratios affect the nonlinear behavior and as can be seen, the turning point where hardening begins for Geometry 1 is quite different than Geometries 2 and 3. For Geometry 2 the shell displays larger lateral displacements but shallow valley at turning point now, Geometry 3 shows smaller lateral displacements but deeper valley at the turning point. Then, in these nonlinear paths it is possible to observe the strong effect of geometry ratios on the nonlinear static behavior of clamped-free cylindrical shells.

Now, the nonlinear forced vibration analysis will be considered, for this, as previously indicated the shell is subjected simultaneously to an axial load $P_{ax}(t)$ and a lateral harmonic radial load $F_{lat}(t)$ acting along $H_L = L/2$, the damping factor is considered $\xi = 0.001$.

First, Figure 4 displays the linear resonance curves obtained for low values of lateral load and increasing small values of axial static load. As can be observed, for small load values, all curves show linear behavior and as can be observed, as the value of axial load is increased, the curves are shifted to the left which means that shells have a reduction of its natural frequency.

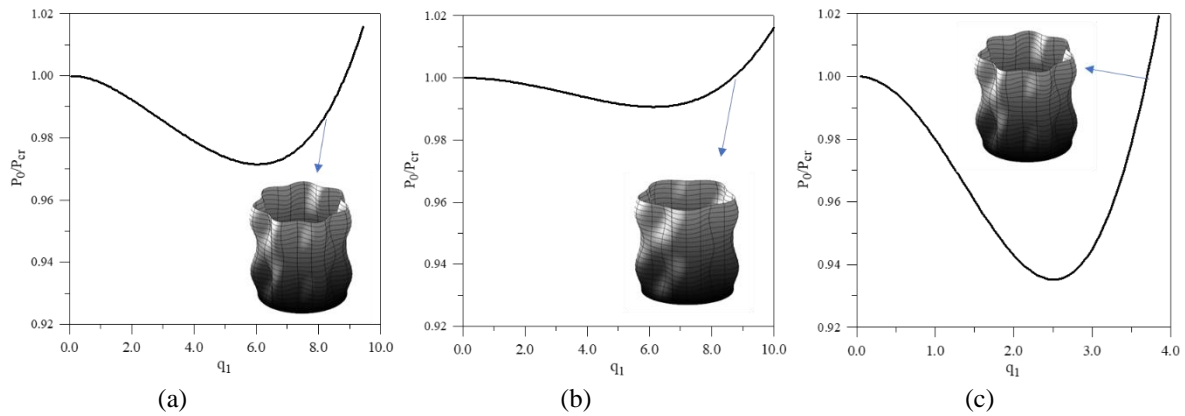


Figure 3. Normalized nonlinear paths for axial static load. a) Geometry 1; b) Geometry 2 and c) Geometry 3.

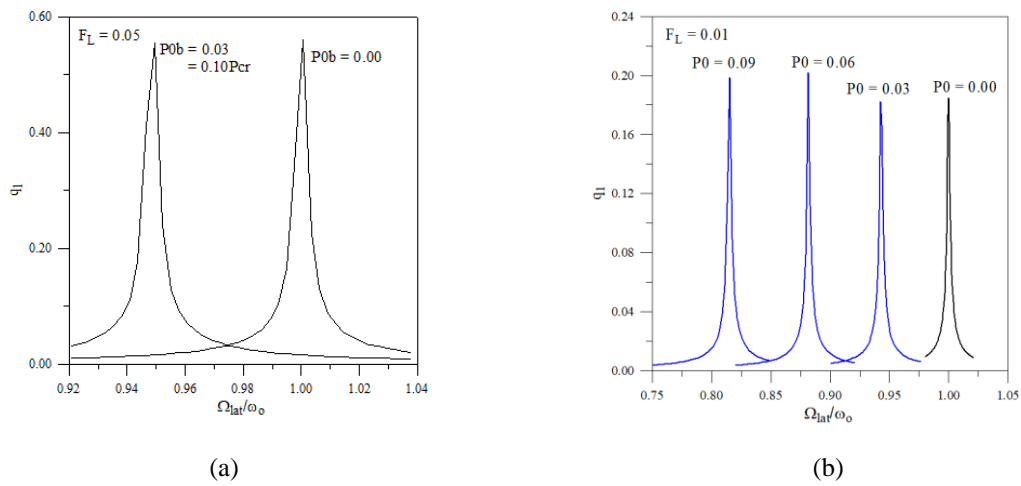


Figure 4. Linear resonance curves for increasing values of axial load. a) Geometry 1; b) Geometry 3.

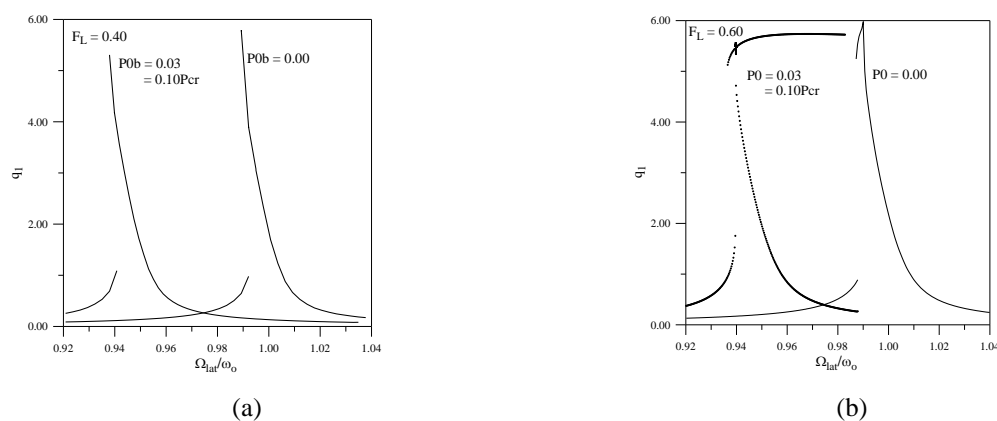


Figure 5. Resonance curves for Geometry 01. a) $F_L = 0.40$ and c) $F_L = 0.60$.

Now, trying to understand the influence of combined loads on the nonlinear dynamic behavior, the nonlinear resonance curves are obtained. Figure 5 depicts the curves for Geometry 1 for increasing values of frequency of lateral load and two values of axial static load. In Fig. 5(a) for lateral load $F_L = 0.40$ and two levels of static axial load $P_0 = 0.0$ and $P_0 = 0.10$ Pcr, both curves display softening behavior with a shifting to the left due to the

increment of axial load, in Fig. 5(b), when lateral load goes up to $F_L = 0.60$, the curves plotted for two values of axial load display softening behavior but, for large amplitude oscillations, the curve for static load $P_0 = 0.10$ Pcr, displays a stable path with hardening characteristics.

Figure 6 depicts the nonlinear resonance curves for Geometry 3, plotted for three levels of lateral load and two values of axial static load. As can be observed, in Fig. 6(a) obtained for $F_L = 0.25$ the resonance curves display softening behavior, in Fig. 6(b) the softening behavior is increased, the nonlinear behavior is also increased and a path with stable hardening behavior is displayed. Now, if the amplitude of lateral load is increased, the resonance curves for two levels of axial load are strongly affected. The resonance curves display hardening behavior and the curve with axial static load, display windows with unstable chaotic vibrations.

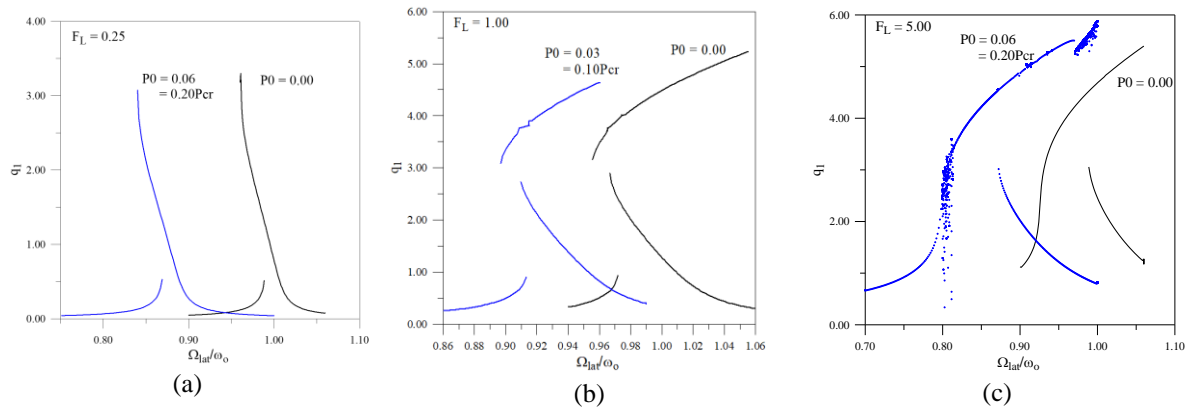


Figure 6. Resonance curves for Geometry 03. a) $F_L = 0.05$; b) $F_L = 1.0$ and c) $F_L = 5.0$, $P_0=0.2P_{cr}$.

Finally, Fig. 7 displays the parametric instability boundary of Geometry 03 obtained for increasing values of amplitude and frequency of axial dynamic load. As can be observed, two valleys which are associated to the natural frequency of the shell can be seen. The principal valley is associated to twice the natural frequency and the secondary valley is associated to the natural frequency. It is also possible to observe that, between the two valleys there is a region where the boundary is not completely defined and displays fractal behavior. Points under the curve represent no steady-state vibrations and points above the boundary, represent large amplitude vibrations of the shell. This boundary indicates how the axial load influences on the nonlinear dynamic response of the shell.

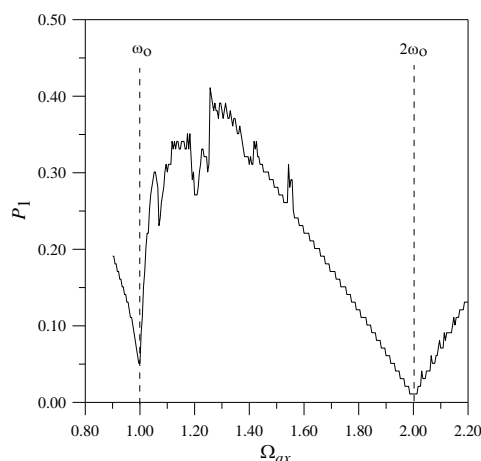


Figure 7. Parametric instability boundary for Geometry 03.

4 Concluding Remarks.

In this work the free and forced nonlinear vibrations of clamped-free elastic cylindrical shells subjected to both lateral and lateral harmonic loads are studied. To model the shell, the Koiter-Sanders nonlinear theory is applied to obtain the strain energy and the field displacements were described by double trigonometric series in both longitudinal and circumferential directions where natural boundary conditions are satisfied.

Three shell geometries (Geometry 1: $L/R=2.0$ and $R/h=944$), (Geometry 2: $L/R=3.0$ and $R/h=800$), (Geometry 3: $L/R=1.0$ and $R/h=200$) were selected to study the influence of geometry ratios on the nonlinear dynamic response, for this, five field displacements were selected, and a convergence study was developed to find the field displacement that generate softening behavior in the frequency-amplitude relations. A series with 15 dof was selected and the resonance curves for increasing values of lateral load were obtained for combinations of axial and lateral loads. As well as the parametric instability boundary

The influence of geometry relations became evident because, depending on its geometry and the values of the load amplitudes, the shell will display linear or softening behavior with small or large amplitude oscillations. For Geometry 1, the shell displays softening behavior and for Geometry 3, the shell displays softening behavior with a hardening path with large amplitude oscillations as well as for large values of load the shell displays hardening behavior with windows of chaotic oscillations.

References

- [1] G. B. Warburton and J. Higgs. "Natural frequencies of thin cantilever shells". *Journal of Sound and Vibration*, vol. 11, pp. 335-338, 1970.
- [2] C. Sharma. "Free vibrations of clamped-free circular cylinders". *Thin-Walled Structures*, vol. 2, pp. 175-193, 1984.
- [3] H. Tottenham and K. Shimizu. "Analysis of the free vibration of cantilever cylindrical thin elastic shells by the matrix progression method". *International Journal of Mechanical Sciences*, vol. 14, pp. 293-310, 1972.
- [4] M. Chiba. "Non-linear hydroelastic vibration of a cantilever cylindrical tank—I. Experiment (empty case)". *International Journal of Non-Linear Mechanics*, vol. 28, pp. 591-599, 1993.
- [5] M. Chiba. "Non-linear hydroelastic vibration of a cantilever cylindrical tank. II Experiment (liquid-filled case)". *International Journal of Non-Linear Mechanics*, vol. 28, pp. 601-612, 1993.
- [6] Ye. Kurylov and M. Amabili. "Nonlinear Vibrations of Clamped-Free Circular Cylindrical Shells". *Journal of Sound and Vibration*, vol. 330, pp. 5363-5381, 2011.